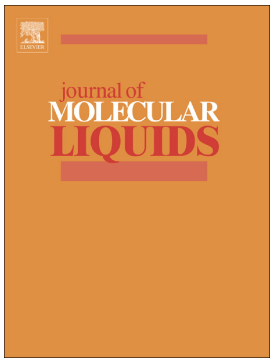

Additivation of MoS2 nanosheets to synthetic poly-alpha-olefins base oils: A theoretical study of nanolubrication

Loukia Maritsa, Sonia Martel, Rocio Barros, Alfredo Bol, Santiago Aparicio

PII: S0167-7322(21)00607-3

DOI: https://doi.org/10.1016/j.molliq.2021.115881

Reference: MOLLIQ 115881

To appear in: *Journal of Molecular Liquids*

Received date: 24 July 2020

Revised date: 3 March 2021

Accepted date: 8 March 2021

Please cite this article as: L. Maritsa, S. Martel, R. Barros, et al., Additivation of MoS2 nanosheets to synthetic poly-alpha-olefins base oils: A theoretical study of nanolubrication, *Journal of Molecular Liquids* (2021), https://doi.org/10.1016/j.molliq.2021.115881

Additivation of MoS_2 nanosheets to synthetic Poly-alpha-olefins base oils: a theoretical study of nanolubrication

Loukia Maritsa[a], Sonia Martel[a], Rocio Barros[a], Alfredo Bol[a,b,*] and Santiago Aparicio[a,c,*]

[a]International Research Center in Critical Raw Materials for Advanced Industrial Technologies (ICCRAM). University of Burgos, 09001 Burgos, Spain

[b]Department of Physics, University of Burgos, 09001 Burgos, Spain

[c]Department of Chemistry, University of Burgos, 09001 Burgos, Spain

[*]Corresponding Authors: alf_bol@ubu.es (A. Bol) and sapar@ubu.es (S. Aparicio)

Abstract

A theoretical study considering Density Functional Theory and classical Molecular Dynamics simulations is reported on the study of the behavior of model poly-α-olefins base oils interacting with 2D MoS_2 monolayers. 2D materials offer a promising route to enhance anti wear and friction reduction. Among them, MoS_2 show a set of specially favourable properties. The objective of the present work is to develop a nanoscopic characterization to show the roots of the use of 2D MoS_2 monolayers as additives that reduce friction and wear with respect to plain lubricants. Three different types of hydrocarbons are considered, including the most relevant features of these oils: linear, star-like and branched compounds. The reported results show a large affinity of the three compounds for the monolayer surface, leading to very efficient adsorption guided by van der Waals interactions as well as by certain charge transfer toward the hydrocarbon. The development of adsorbed layers on the surface leads to changes in the base oil properties although being concentrated in a region close to the monolayer, with lower effects at larger distances. The presence of hydrocarbons with very different geometries hinders highly ordered molecular packing beyond the layer in direct contact with the surface. Nevertheless, the rearrangements on top of the MoS_2 surface will lead to large changes in the base oil behavior for lubrication purposes, enhancing tribological and anti-wear properties of MoS_2 nanosheet additivated poly-α-olefins base oils.

Keywords: molybdenum disulfide; 2D materials; liquid lubrication: olefin lubricants; molecular modelling.

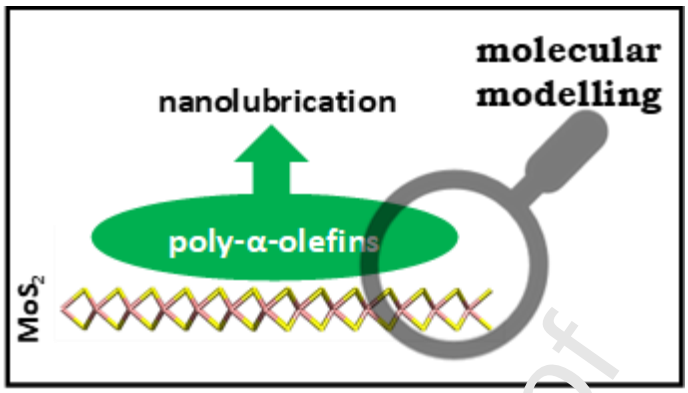

Graphical abstract

Introduction

The reduction of friction and wear of machine parts is of great relevance not only because of technological purposes but also from a sustainability viewpoint considering that 20 % of the world's total energy consumption is used to overcome friction [1]. The purpose of improving lubrication, and thus reducing energy losses, may be fulfilled using new technologies for surface treatment, new materials and lubricants. A suitable approach consists in the modification of traditional lubricant base oils by the addition of nanoparticle additives, which have showed to improve the tribological behavior of lubricants [2].

The use of Trivalent Metal Dichalcogenides (TMDs), especially MoS_2, as nanoadditives for base lubricant oils has been considered in the literature [3,4]. Many different geometries for TMDs nanoadditives have been proposed starting from nanosheets (hydrothermally synthesized [5] or electrochemically exfoliated [6]) to complex structures like flower-like [7] or spherical nanoparticles [8], and advanced structures like nano-MoS_2 quantum dots [9]. MoS_2 nanoparticles have proved to reduce friction and wear in concentrations below 2 wt% for different types of base oils [10]. In particular, two-dimensional MoS_2 monolayers have proved to be successful nanomaterials for improving, modifying and controlling base oil properties [11,12,6]. These 2D nanoadditives have showed remarkable lubrication improvements; for 2D hydrothermally synthesized MoS_2, decreases up to 60% in the coefficient of friction and 7% wear scar diameter with low nanoadditives concentrations (0.05 wt%) [13]. for 2D electrochemically exfoliated MoS_2, decreases up to 10% in the coefficient of friction and 42% wear scar width with the same low concentrations [6]. 2D MoS_2 nanosheets have exhibited suitable dispersing ability in base oils [14] [6], with the friction and wear reduction produced by the suitable nanomaterial penetration into the contact areas, thus leading to the formation of thick tribofilms inside the wear tracks and the prominent tribological performance of the two-dimensional MoS_2 nanosheets.

The probed performance of 2D MoS_2 monolayers as nanoadditives requires a suitable characterization of the mechanism of base oil – nanosheets interactions to show the changes in the lubricant properties in presence of the nanoparticles. This understanding will allow to improve the lubricant formulations as a function of the type and concentration of the additives, and it will show the nanoscopic basis of lubrication mechanisms. Although the available experimental studies have partially

showed the properties of the oils + MoS_2 nanofluids, thus showing the changes in the thermophysical properties of the oil in presence of the nanoadditives as well as proposing possible lubrication mechanism [6, 15 , 16] a detailed nanoscopic characterization is still absent. For this purpose, molecular modelling studies are a suitable tool for characterizing the nature and structure of the considered nanofluids, providing nanoscopic details not reachable through most of the experimental researches. Despite the relevance of molecular simulation studies, the available literature is scarce. A previous study reported by our research group studied the interaction of hydrocarbons (n-octane) with 2D MoS_2 monolayers, thus showing an impressive rearrangement of the fluid in the vicinity of the monolayer surface leading to a quasi-smectic liquid crystal behavior which would be on the roots of the base oil modifications because of the nanoparticles presence [17]. Although this previous study probed the fundamentals of hydrocarbon – monolayers interactions, the composition of base oils is far more complex, and thus the study of complex hydrocarbon mixtures is required to show the real behavior of MoS_2 monolayers in real lubricants.

Model

Poly-α-olefin (PAO) synthetic lubricants are largely relevant oils for the industry [18], for example for synthetic motor oil basestock [19], and thus their consideration for the study of MoS_2 monolayers as additives is highly relevant. A model of PAO synthetic lubricants was developed by Kioupis et al. [20] for their molecular dynamics (MD) simulations. They considered three different isomers to represent the most relevant molecular features of these base oils: *i*) n-octadecane (C18), to represent linear long n-alkanes, *ii*) 7-butyl-tetradecane (C14_C4), used to model star-like components of the oil with some degree of molecular branching, and *iii*) 4,5,6,7-tetraethyl-decane (C10_4C2), to consider highly branched compounds in the oil (Figure 1). It should be remarked that for base oil components, linear hydrocarbons although being largely present are not very good lubricant agents because of their high pour points, thus the introduction of branched hydrocarbons lower the oil pour points although increases oils viscosity. Therefore, a balance between linear and branched compounds is considered during base oils formulations. Previous theoretical studies have considered

the behavior or graphene 2D materials on PAOs lubricant oils [21], showing the modifications of the oil by the presence of nanosheets and probing the suitability of 2D nanomaterials for modifying PAOs base oils properties.

The required nanoscopic characterization of PAO – 2D MoS_2 nanofluids is reported in this work by using a combined theoretical study using Density Functional Theory (DFT) and classical MD simulations considering the three PAO components as reported in Figure 1. DFT studies on the PAOs – monolayer surface interactions provide structural and energy characterization of the interaction of the PAOs with the surface, thus characterizing the main features of PAOs adsorption and main features of PAOs modification because of the monolayer presence. Further characterization, in terms of size and time, is developed by using MD, in which a mixture of the three PAO components (x = 0.33, for the three PAOs, with x standing for mole fraction) in contact with the monolayer surface is analyzed. This multiscale approach provides a detailed characterization of the main features of lubricants – 2D MoS_2 monolayers, thus providing the characterization in terms of base oil structural changes, adsorption, interface behavior and systems energy. The reported results will allow to advance in the knowledge of 2D TMDs as additives for improving oils performance, thus enhacing lubrication processes.

Methods

SIESTA 3.2 package [22] was used for DFT calculations. The theoretical level combined generalized gradient approximation (GGA) with Perdew-Burke-Ernzerhof (PBE) [23] functional and norm-conserving pseudopotentials, with Troullier–Martins parameterization [24]. Numerical double-z polarized (DZP) basis sets were considered. The Grimme's approach [25] was applied for including van der Waals dispersion interactions. A 2D MoS_2 monolayer with 147 atoms and 22.1228 × 22.1228 $Å^2$ dimensions was used with 20 Å vacuum layer on top of it. Single PAO molecules were initially placed at 3 Å on top of the monolayer and they were relaxed using the conjugated gradient method (force convergence criterion of 0.04 $eV \cdot Å^{-1}$) with self-consistent field equations solved to $1 \cdot 10^{-4}$ eV. 9 × 7 × 1 Monkhorst-Pack grid [26]

with a cut-off of 400 Ry was considered. The strength of PAOs adsorption on the monolayer surface was quantified using the interaction energies, Δ*E*:

$$\Delta E = E_{cluster} - E_{MoS_2} - E_{PAO} \quad (1)$$

where $E_{cluster}$, E_{MoS_2} *and* E_{PAO} are the energy for system formed by PAO - MoS_2, for the isolated MoS_2, and for PAO isolated molecules, respectively.

MDynaMix v.5.2 package [27] was used to carry out classical MD simulations. For MoS_2, Sresht et al. [28] force field was considered, and it has showed to be suitable for describing MoS_2 – hydrocarbon interactions [16]. The PAOs molecules were described using OPLS-AA force field [29]. A MoS_2 monolayer composed of 756 atoms (49.2×44.3 Å^2) was placed in the *xy* plane. The systems considered for MD simulations were i) pure PAO liquid layers (250 PAO molecules) on top of MoS_2 monolayer, considering pure C18, C14_C4 or C10_4C2 molecules, ii) a PAO liquid layer on top of MoS_2 monolayer composed by a mixture of C18 + C14_C4 + C10_4C2 (*x* = 0.33, with *x* being mole fraction and 255 total molecules). All the systems have 250 Å in the direction perpendicular to the monolayer surface, thus monolayer – PAO and monolayer – vacuum interfaces are present in the simulated systems. Initial simulation boxes were built using Packmol program [30]. Periodic boundary conditions in the three space directions were considered. MD simulations in the NVT ensemble at 293 K for 50 ns were carried out. The systems temperature was controlled with the Nosé-Hoover method. Ewald method was applied for Coulombic interactions (15 Å cut-off). Lennard-Jones contributions calculated with a 15 Å cut-off, and Lorentz-Berthelot mixing rules. Tuckerman–Berne double time step algorithm [31] (1 and 0.1 fs for long and short time steps) was considered for solving the equations of motion. The Data analysis s was carried out with VMD [32], TRAVIS [33] and VESTA [34] softwares.

Results and Discussion

DFT Results. The systems considered for DFT calculations involve single PAO molecules placed on top of the MoS_2 monolayer, which were relaxed to infer the most favorable configuration of interaction between the PAO and the surface, thus providing the fundamentals of the mechanism(s) of adsorption. Results in Figure 2 show the lowest energy conformation of PAO + MoS_2 systems for C18, C14_C4 and

C10_4C2. The values reported for Δ*E* show large affinity for the monolayer surface for the three considered PAOs following the ordering C18 > C14_C4 > C10_C4C2. The geometry (branching) of the PAO molecule has a large effect both on the strength of the interaction with the MoS_2 surface as well as in the molecular arrangement on the surface. In a previous study, the adsorption of n-octane molecule on MoS_2 was studied by using DFT showing a Δ*E* = - 1.8 eV [16]. Results in Figure 2a for C18 show Δ*E* = -4.6 eV, which is 2.6 times larger than for n-octane, considering that C18 has 2.3 times C atoms than n-octane, the increase in Δ*E* would correspond to the increase of hydrocarbon – monolayer van der Waals contacts, which are the main components guiding the adsorption on the surface. Likewise, the C18 to surface distance (3.35 Å) is almost the same as for n-octane (3.2 Å [16]), thus confirming the same interaction mechanism for linear n-alkanes. The molecular orientation of C18 on the monolayer surface, Figure 2a, confirms an almost perfect parallel arrangement regarding the top S atoms, which will increase van der Waals interactions. Nevertheless, the van der Waals like interactions are not the only relevant feature determining C18 interaction with the surface, the calculated Hirshfeld charges show that C18 is partially charged upon adsorption on the surface, which will lead to C18 – surface relevant electrostatic interactions. This effect is not dependent on the considered charge model, analogous results were inferred using the Voronoi method. The different terms contributing to the total Δ*E* are reported in Figure 3. These results confirm that van der Waals interactions, described in this work using Grimme's method, have a prevailing role for the C18 adsorption, being a 36 % of the total ΔE. In fact, energy associated to van der Waals interaction is the only energy term with favorable monotonic contribution to the adsorption while the other three terms show a more complex behavior. They are favorable and unfavorable to adsorption, depending on the hydrocarbon geometry and, as it will be shown later, the electronic density cloud. Furthermore, these results agree with Fourier Transform Infrared spectroscopy that reveal that no new spectral peaks or shifts are found for the additivated lubricants compared to the plain engine base oil, indicating that no chemical bounds are formed [6].

The development of branching in PAOs changes the mechanism of interaction with the surface, specially for high degree of branching. Results in Figure 2 for C14_C4 and C10_4C2 show that branching decreases Δ*E*, with the larger decreases with larger

degree of branching. Although C14_C4 and C10_4C2 still show remarkable affinities for the monolayer surface, as confirmed by their Δ*E* values, these are lower than those for C18 in spite of having the same number of C atoms. In the case of the star-like C14_4C4 structure, the molecule is still adsorbed in a slightly skewed orientation on the surface showing large Δ*E*, but the distance to the surface increases in comparison with C18 as well as the charge on the PAO, thus justifying the lower Δ*E*. Nevertheless, the van der Waals contribution is still the main component of C14_C4 interaction with the monolayer, with the other terms to the total Δ*E* also decreasing when compared with C18, Figure 3. In the case of largely branched C10_4C2 PAO, the lower Δ*E* is clearly justified by the molecular arrangement reported in Figure 2c. The C10_4C2 molecule adopts a non-parallel arrangement on the MoS_2 surface, which decreases the average molecular distance to the monolayer, thus decreasing both the van der Waals interactions as well as the surface to PAO charge transfer and weakening adsorption ion the surface. Therefore, the PAOs adsorption mechanism is largely dependent on the degree of branching, with decreasing strengths of adsorption when the molecular structure deviates from the linearity. This effect would guide the behavior of lubricants on the surface because branched and non—branched PAOs are included in the formulations to improve performance.

The adsorption of PAOs on the monolayers may lead to changes in molecular properties and geometries upon adsorption. The average carbon – carbon bond distance is quantified for the three studied PAOs when adsorbed on the surface and reported in Figure 4. The average C-C distance for isolated PAOs (i.e. in gas phase, non-adsorbed) is 1.53 Å, thus results in Figure 4 show very minor changes upon adsorption, a slight trend to increase C-C bond distance is inferred, especially for branched compounds but the features of PAOs are maintained upon adsorption in spite of the strong interaction with the MoS_2 surface. The PAOs – 2D MoS_2 interactions upon adsorption may produce changes in the monolayer properties. This possible effect was quantified by the Density of States (DOS) as reported in Figure 5. A first inspection of DOS in Figure 5 show minor changes when comparing clean monolayer with those including the adsorbed PAOs both for linear and branched hydrocarbons. The most relevant features are maintained, with the only relevant change being produced by the decrease in the band gap, especially when branched hydrocarbons are present. The

band gap calculated in this work for pristine 2D MoS_2 monolayer is 1.73 eV, which agrees with theoretical values reported in the literature (1.66 [35] to 1.9 eV [36], depending on the considered theoretical approach) and are also in suitable agreement with experimental value (1.8 eV [34]). For C18 + MoS_2, the band gap decreases to 1.47 eV, and for C14_C4 and C10_4C2 band gaps of 1.18 and 0.67 eV, respectively, are obtained.

The changes in the band gap as well as the reported monolayer to PAO charge transfer indicate that, apart of van der Waals like interactions, there should be relevant interactions affecting the electronic density upon PAOs adsorption. These effects are analyzed in Figure 6 showing the electronic density distribution along a plane perpendicular to the monolayer surface. Results in Figures 6a and 6b show electron density profiles along the H and C atoms of C18 molecule, perpendicular to the monolayer surface. In the case of H atoms, Figure 6a, which are closer to the surface than C ones (Figure 2a) there is a clear overlapping between the electronic distributions on the surface and those corresponding to the PAOs. The reported results show that H atoms close to the surface are efficiently interacting through shared electronic density regions, through which the charge transfer toward the PAO is produced, thus leading to the charges reported in Figure 2a. The electronic density along a plane perpendicular to the surface through the C atoms show a minor overlapping with the underlying monolayer, although some interaction is inferred it is clear from Figures 6a and 6b that the interaction is mainly produced through the H atoms. In the case of branched molecules, Figure 6c for C14_C4, the arrangement of PAO molecules, not so perfectly planar as for linear C18, allows a more efficient interaction through the C atoms, with an increase in the overlapping of electronic density regions (Figures 6b and 6c), thus leading to charge transfer not only through the H atoms but also through some of the C atoms. This will justify the large charge transfer reported for C14_C4, Figure 2b, in spite of the lower molecular planarity on the surface upon adsorption in comparison with C18. In the case of highly branched C10_4C2, the low charge transfer, Figure 2c, show minor overlapping of electronic density regions because of the non-planarity of PAO molecule upon adsorption. These results for electron density evolution are confirmed in Figure 7 where the electronic density in the middle of the region of monolayer – PAO interaction are reported.

Results for C18 and C14_C4_ show high electron density below each PAO molecule, Figures 7a and 7b, thus showing overlapping and sharing of electronic clouds, whereas low density is inferred for C10_4C2, Figure 7c

MD Results. The DFT results reported in the previous section show the main features of PAO molecules interacting with MoS_2 monolayer surface. Nevertheless, the behavior of MoS_2 monolayers as additives to PAO lubricant oils requires to consider additional effect because of the presence of PAO liquid layers, which are not considered in DFT calculations, and which can be reached through MD simulations. To attain a systematic picture of the behavior of PAOs with regard to the considered surface, first PAO liquid layers composed by a single type of PAO where put in contact with the monolayer, and then simulations considering a PAO mixture (C18 + C14_C4 + C10_4C2) was considered. In this way, particular effects rising from each type of molecule are inferred as well as well as additional effects by the simultaneous presence of the three types of PAOs, i.e. possible cooperativity, synergistic or additional effects as present in the real base oil.

Molecular density profiles along a plane perpendicular to the monolayer surface are reported in Figure 8 for the three systems considering pure PAOs in contact with 2D MoS_2. Results in Figure 8a shows a completely different behavior for C18 in comparison with C14_C4 and C10_4C2. The distribution of C18 is characterized by the presence of successive adsorbed layers on top of the monolayer surface. The first layer is the most clearly defined with the number density peaks intensity being damped with increasing distance to the surface, but nine well defined consecutive layers are inferred. This effect was previously reported for a shorter hydrocarbon, n-octane [16], and it is a consequence of the large affinity of linear n-alkane molecules for the MoS_2 surface as well as for the arrangement of C18 molecules on top of the surface, which allows efficient C18 - surface interactions as well as C18 – C18 ones. Results in Figure 8b show the distribution of C18 on top of the monolayer, and although the first layer is perfectly defined, additional layers are less defined, especially when compared with previous results for n-octane, which showed a quasi-smectic like behavior [16] not present for long C18 hydrocarbon. Therefore, a highly structured fluid is inferred for C18 on top of the monolayer but the structuring is less remarkable than for shorter hydrocarbons. The parallel orientation of C18 molecule

with regard with the monolayer surface along the simulations is confirmed in Figure 9 using the angle distribution. In the case of branched C14_C4 and C10_4C2 a first strongly adsorbed layer is inferred, Figures 8a, 8b and 8c, but further ordering is limited to a second adsorbed layer without additional perturbation of the liquid. Likewise, the orientation on the first layer is not prevailing parallel to the surface in contrast with the C18 distribution. These results agree with DFT orientations reported in the previous section and show the disrupting effect of branching in PAOs with regard to the orientation on the surface and liquid rearrangements.

The strength of pure PAOs – monolayer interactions is quantified from MD simulations, Figure 10. Larger, E_{inter} values for C18 are inferred but efficient interaction for C14_C4 and C10_4C2 are also reported. Therefore, although the parallel arrangement of C18 on the surface allows larger van der Waals interactions, i.e. stronger adsorption, in the case of branched hydrocarbons the less oriented structuring do not avoid efficient interaction with the surface, thus allowing efficient adsorption although limited to the layers in direct contact with the surface.

Once the PAOs molecules are adsorbed on the monolayer surface their distribution is completely different to those in bulk liquid phases. In the case of C18, radial distribution functions, RDFs, Figure 11a show that C18 molecules are closely packed to neighbor molecules. The arrangement reported in Figure 11b shows localized domains with C18 molecules, with parallel arrangements to the surface, and they are also adopting parallel orientations between them, thus leading to efficient C18 – C18 interactions. This efficient self-aggregation of C18 molecules also favors the stabilization of the adsorbed layers beyond the strong affinity for the surface. In the case of branched compounds, RDFs do not show efficient self-aggregation on the adsorbed layer, especially for C10_4C2. The branching of PAOs hinders efficient self-interaction, leading to lower PAOs density, Figure 8a, and thus to less stable adsorbed layers.

The larger interaction energy between the PAOs and the monolayer surface, combined with the PAO – PAO self-interactions upon adsorption, especially for C18, should modify the dynamic properties of the PAOs in comparison with those molecules in the bulk liquid phases. Self-diffusion coefficients, *D*, were calculated from mean square displacements, *msd*, and Einstein's equation. Values reported in Figure 12 show

lower diffusion rates for C18 in comparison with branched PAOs. Additionally, the strong linear correlation between *D* values and E_{inter} confirms that the stronger the affinity of the PAOs for the surface the slower the molecular diffusion. Therefore, C18 showing the larger orientation on the surface because of its strong affinity leads to lower *D* values when compared with branched PAOs. Nevertheless, considering that branched PAOs have suitable affinity for the monolayer surface, their molecular mobility is also low once they are adsorbed. These results confirm that the modification of base oil properties would stand not only on the behavior of C18 (i.e. linear compounds) but also on the branched ones.

Results in previous section considered the behavior of pure PAOs on the monolayer surfaces, but the modelling or a realistic base oil was developed using a C18 + C14_C4 + C10_4C2 mixture, with the same content for all the considered PAOs (*x*=0.33). Number density profiles reported in Figure 13 shows a first adsorbed layer in contact with the surface with presence of the three PAOs. The composition of this first layer is slightly different to that for the bulk liquid phase, with an enrichment in C18 and mainly in C14_C4 and a lower content for C10_4C2. Likewise, the ordering because in the mixture is well extended beyond the first layer, and although being less remarkable than for neat C18 shows that the simultaneous presence of the three components leads to larger disruption of liquid structuring in comparison with pure branched PAOs. Therefore, a cooperative effect is inferred which show that in the case of real base oils the disruption of the oil structuring would be extended beyond the region in close contact with MoS_2 nanosheets as well as indicating that branched hydrocarbons are also adsorbed on the surface despite of their lower affinity for the monolayers. The interaction energies for the adsorbed mixture are reported in Figure 14. It should be remarked that larger values are obtained for C14_C4, which agrees with the enrichment in this compound reported in Figure 13 for the first adsorbed layer. Nevertheless, the three PAOs show strong interactions with the surface thus confirming suitable adsorption. Additionally, results of E_{inter} for PAO – PAO interactions show that homo and heteroassociations are developed upon adsorption although being weaker than PAO – monolayer ones. RDFs reported in Figure 15 show that C18 molecules maintain their trend to be self associated and the branching of C14_C4 and C10_4C2 leads to less ordered self and heteoassociations upon mixture adsorption.

Nevertheless, the suitability of each type of PAO to be or self-associated or to develop heteroassociations with other types of PAOs allows efficient adsorption for all the mixture components, no preferential PAO interaction seems to be developed and the simultaneous presence of all the mixture component in the adsorbed layers confirm that the studied model base oil interacts efficiently with the nanomaterial with large modifications on the oil properties.

From the experimental point of view Guimarey et al. [6] have shown that additivation of 2D MoS_2 to a PAO based oil (commercial SAE 5W-30) decreases kinematic viscosity (around a 6 % for different MoS_2 concentrations), decreases coefficient of friction (10 % for 0.05 wt %) and decreases width (30 % of mean reduction for different concentrations) and depth (45 % of mean reduction for different concentrations) of wear scars obtained during rotational friction tests. They explain this good tribological behaviour because of efficient film formation and polishing effect (roughness reduction of the lubricating surface by nanoparticle-assisted abrasion). Our results suggest that not only substantial absorption of PAOs molecules but also the structuring of the liquid induced by the presence of 2D MoS_2 is the key mechanism of tribofilm formation and boundary regime lubrication improvements.

Conclusions

The properties of selected poly-α-olefins on 2D MoS_2 monolayers are studied by using a combined computational approach using Density Functional Theory and classical molecular dynamics simulations to analyse the behaviour of base oils modifications because of the nanomaterial presence for lubrication purposes. Studied system comprise both pure poly-α-olefins and a mixture containing linear and branched compounds to mimic the behaviour of real oils. The reported results show a large affinity of the considered poly-α-olefins for the MoS_2 surface leading to large modifications of the fluid structuring in the vicinity of the monolayers. Although larger modifications are inferred for linear hydrocarbons, branched compounds are also efficiently adsorbed on the monolayer surface. Likewise, the simultaneous presence of branched and linear poly-α-olefins reinforces the adsorption on the surface, leading to

a cooperativity effect because of the simultaneous development of efficient interactions with the surface and between the hydrocarbons. The reported results provide a nanoscopic vision of the behaviour of MoS_2 monolayers confirming that large modifications are produced in the base oils leading to layering in the vicinity of the surfaces, which will favour lubrication upon adsorption of the oil on the nanomaterial and suggesting an explanation of the experimentally observed results.

Acknowledgements

This work was funded by European Union (H2020-MSCA-ITN-2016-SOLUTION-GA-721642 project). We also acknowledge SCAYLE (Supercomputación Castilla y León) for providing supercomputing facilities. The statements made herein are solely the responsibility of the authors. The authors declare no competing interests.

Author Statement

The individual contributions to the paper are as follows:

- Loukia Maritsa. University of Burgos. Spain. CONTRIBUTION: investigation, methodology, data curation, writing original draft.
- Sonia Martel. University of Burgos. Spain. CONTRIBUTION: conceptualization, methodology, project administration, resources.
- Rocio Barros. University of Burgos. Spain. CONTRIBUTION: conceptualization, methodology, project administration, resources
- Prof. A. Bol. University of Burgos. Spain. CONTRIBUTION: conceptualization, methodology, funding acquisition, supervision, project administration, resources, writing-original draft, writing-revised draft.
- Prof. S. Aparicio. University of Burgos. Spain. CONTRIBUTION: conceptualization, methodology, funding acquisition, project administration, resources, supervision, writing-original draft, writing-revised draft.

Conflicts of Interests Statement

The authors whose names are listed immediately below declare that they have no known competing financial interests or personal relationships that could have appeared to influence the work reported in this paper.

Figure 1. Molecules considered in this work for the study of PAOs.

Figure 2. DFT results for the adsorption of a single {C18 or C14_C4 or C10_4C2} molecule on 2D MoS_2 surface. Interaction energy, ΔE, and the carbon to top sulphur layer distance (blue arrows and labels) are reported. For the reported distances, the average values for all the PAOs carbon atoms are reported with the corresponding standard deviation. Total charge on PAO molecules are reported (red labels) according to Hirshfeld, q_{HIR}, and Voronoi, q_{VOR}, methods.

Figure 3. Contributions to the total interaction energy of a single {C18 or C14_C4 or C10_4C2} molecule on 2D MoS_2 surface. Contributions: kinetic (Pauli repulsion), exchange correlation, electrostatic (sum of Hartree contribution plus ion−ion and ion− electron terms), and molecular mechanics (Grimme's contribution).

Figure 4. Evolution of average C-C bond distance, $d_{C\text{-}C}$, along DFT geometry optimization for {C18 or C14_C4 or C10_4C2} molecule on 2D MoS_2 surface. Average values are reported inside the panel.

Figure 5. Total density of states for {C18 or C14_C4 or C10_4C2} molecule on 2D MoS_2 surface.

Figure 6. Electronic density for (a,b) C18 or (c) C14_C4 molecule on 2D MoS_2. Results are reported for a plane perpendicular to the 2D MoS_2 surface through (a) H or (b,c) C atoms. White arrows indicate the region below the PAO interacting (green areas) with the S atoms in the 2D MoS_2 surface.

Figure 7. Electronic density for (a) C18, (b) C14_C4 or (c) C10_4C2 molecule on 2D MoS_2. Results are reported for a plane (p_2) parallel to the 2D MoS_2 surface for a distance in the middle between sulfur and hydrogen atoms.

Figure 8. (a) Number density profiles, ρ, in the direction perpendicular to the MoS_2 surface (d=0 stands for the position of the top S atoms) for {C18 or C14_C4 or C10_4C2} + 2D MoS_2 systems. Results in panels b to d show snapshots after 100 ns of MD simulations for the same systems as in panel a. Color code in panels b to d: the first adsorbed layer is indicated in (blue) C18, (red) C14_C4 or (green) C10_4C2; (cyan) molecules beyond the first adsorbed layers. Only C atoms are plotted in panels b to d for the sake of visibility.

Figure 9. Orientation of PAO molecules on MoS_2 surface quantified by the distribution of the reported orientation angle, φ, for {C18 or C14_C4 or C10_4C2} + 2D MoS_2 systems.

Figure 10. Intermolecular interaction energy, E_{inter}, for PAO – MoS_2 interactions (sum of Lennard-Jones and coulombic contributions) for neat PAOs. Neat stands for {C18 or C14_C4 or C10_4C2} + 2D MoS_2.

Figure 11. (a) Center-of-mass radial distribution functions, $g(r)$, for PAO – PAO pairs in the first adsorbed layer on MoS_2 surface in {C18 or C14_C4 or C10_4C2} + 2D MoS_2 systems. Results in panels b to d show snapshots after 100 ns of MD simulations for the same systems as in panel a showing PAO molecules in the first adsorbed layer. Color code in panels b to d: the first adsorbed layer is indicated in (blue) C18, (red) C14_C4 or (green) C10_4C2. Only C atoms are plotted in panels b to d for the sake of visibility.

Figure 12. Relationship between Intermolecular interaction energy, E_{inter}, and self-diffusion coefficient, D, of PAO molecules in the first adsorbed layer on MoS_2 surface. in {C18 or C14_C4 or C10_4C2} + 2D MoS_2 systems. D values are calculated for diffusion on the MoS_2 surface from mean square displacements and Einstein's equation.

Figure 13. Number density profiles, ρ, in the direction perpendicular to the MoS_2 surface (d=0 stands for the position of the top S atoms) for {(x=0.33) C18 + (x=0.33) C14_C4 + (x=0.33) C10_4C2} mixture (x stand for mole fraction) + 2D MoS_2 systems. Values inside the figure show the mole fraction in the first adsorbed layer (x_{1st}) for each component.

Figure 14. Intermolecular interaction energy, E_{inter} (sum of Lennard-Jones and coulombic contributions), for (full bars) PAO – MoS_2 interactions, (dashed bars) PAO – PAO homoassociations, and (black bars)

PAO – PAO heteroassociations for {(x=0.33) C18 + (x=0.33) C14_C4 + (x=0.33) C10_4C2} mixture (x stand for mole fraction) + 2D MoS_2 systems.

Figure 15. Center-of-mass radial distribution functions, $g(r)$, for PAO – PAO pairs in the first adsorbed layer on MoS_2 surface for {(x=0.33) C18 + (x=0.33) C14_C4 + (x=0.33) C10_4C2} mixture (x stand for mole fraction) + 2D MoS_2 systems. Results in panels a and b show values for homo and heteroassociations, repectively.

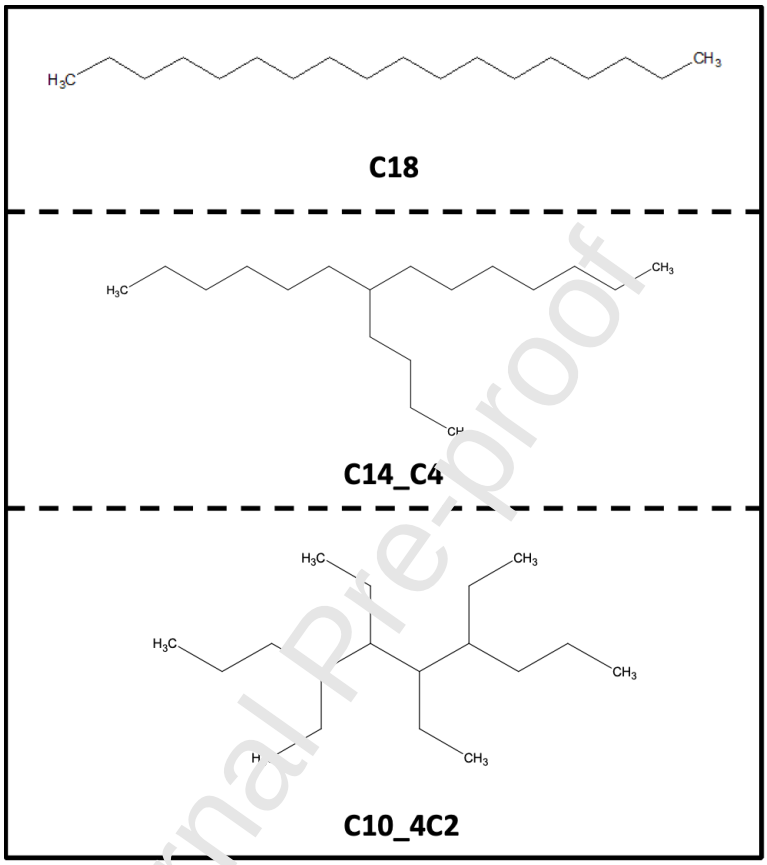

Figure 1

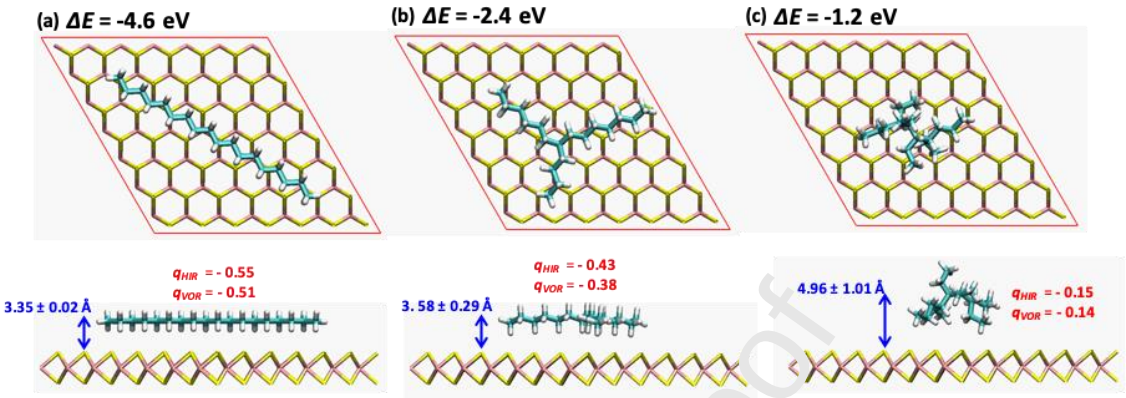

Figure 2

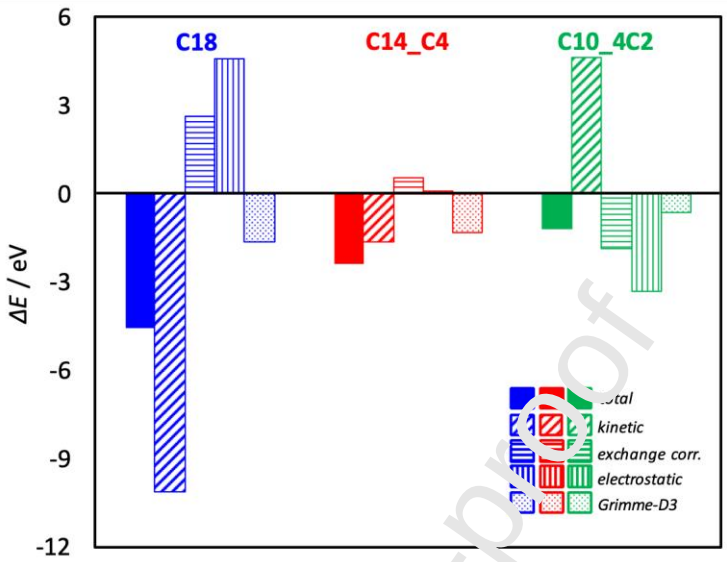

Figure 3

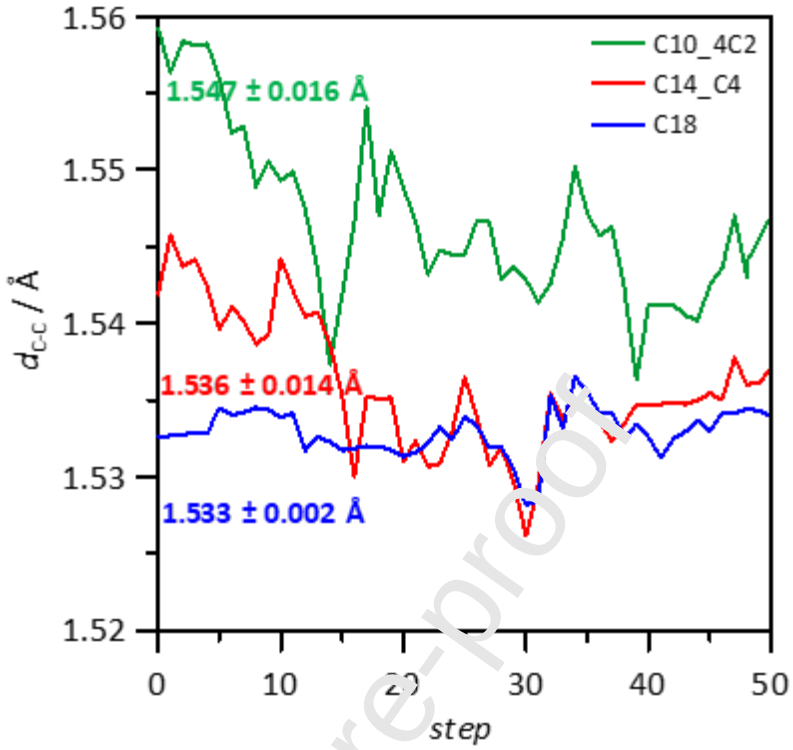

Figure 4

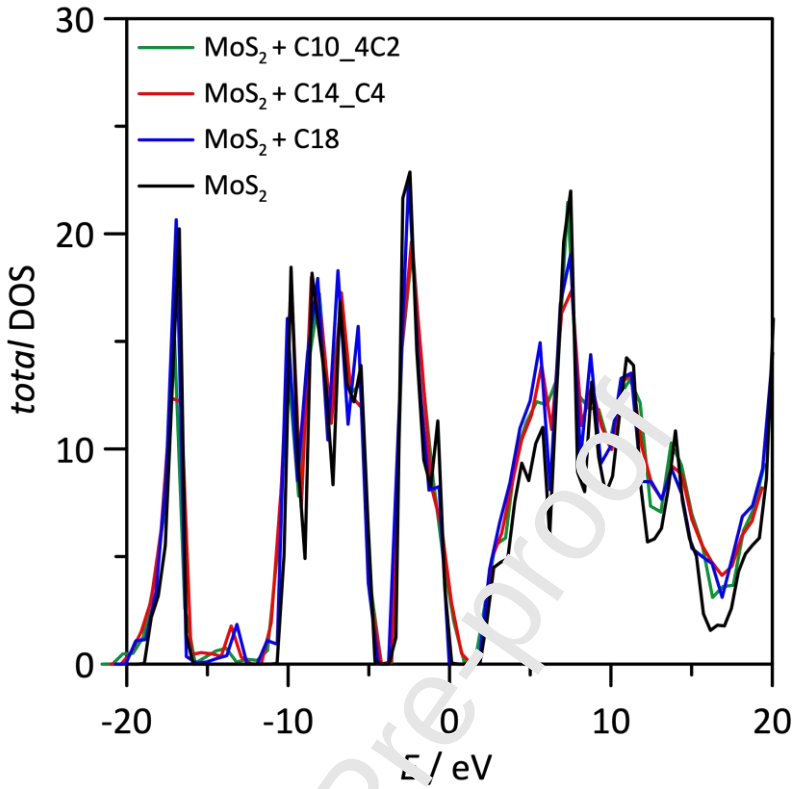

Figure 5

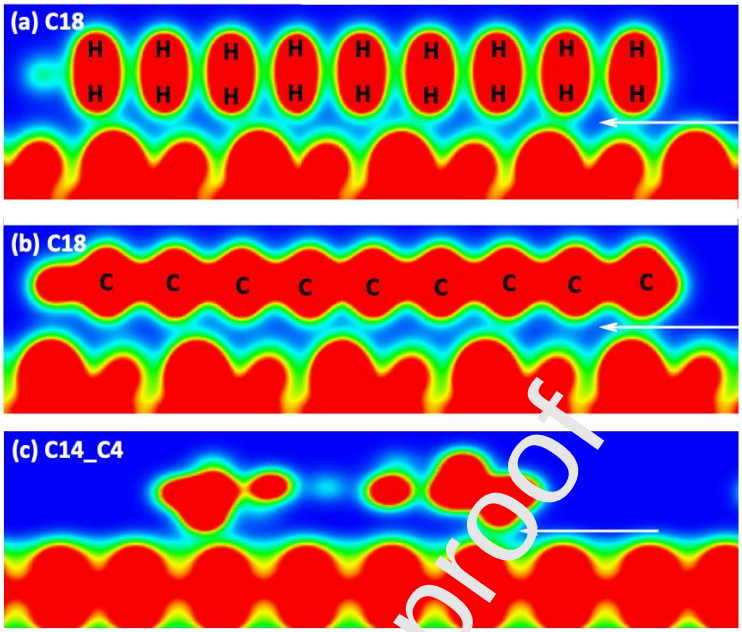

Figure 5

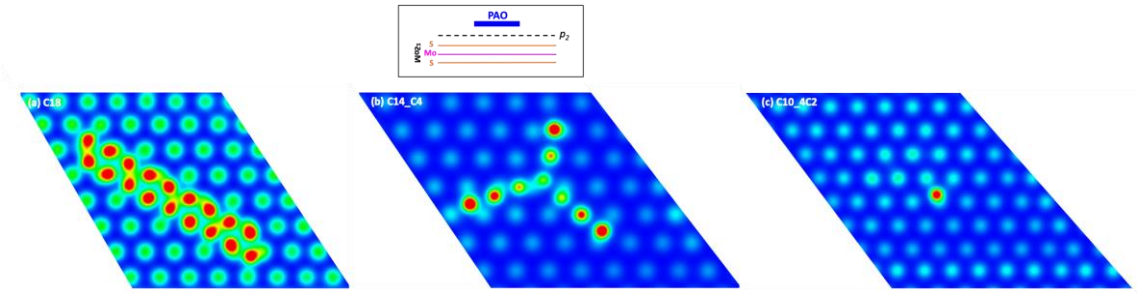

Figure 7

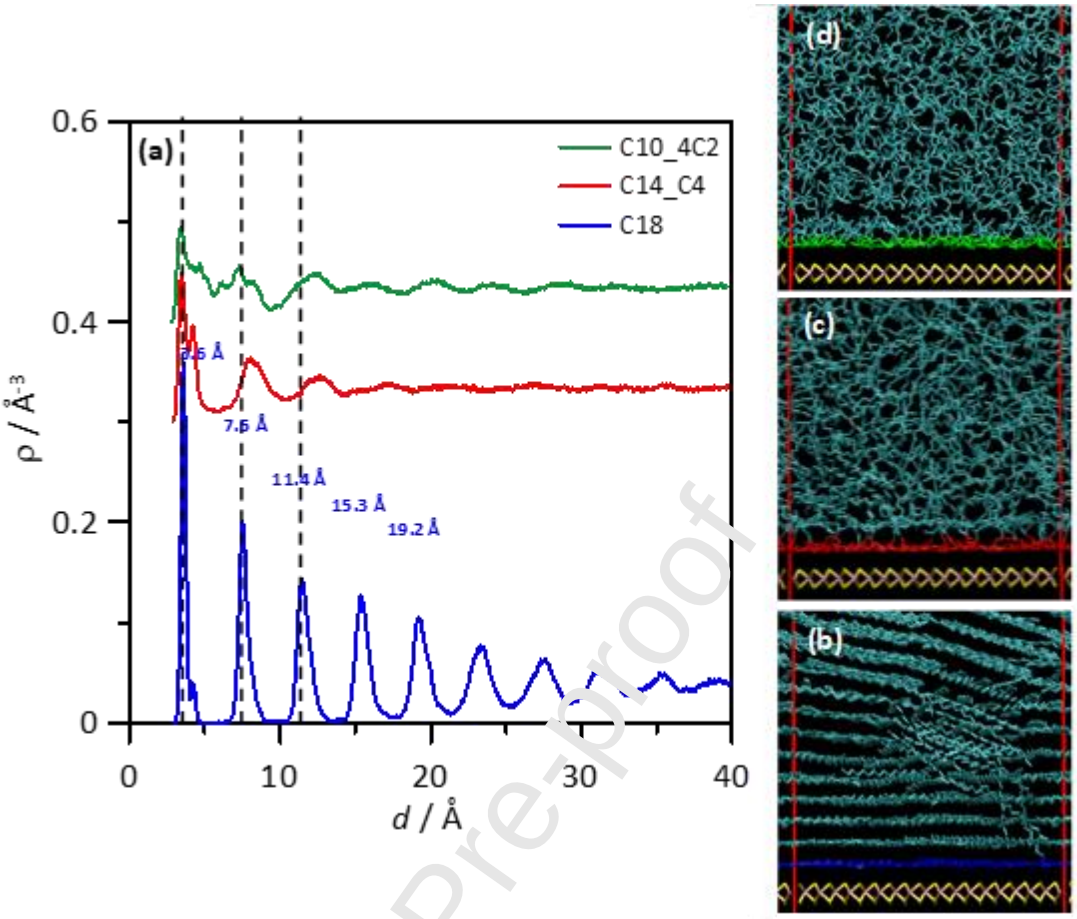

Figure 8

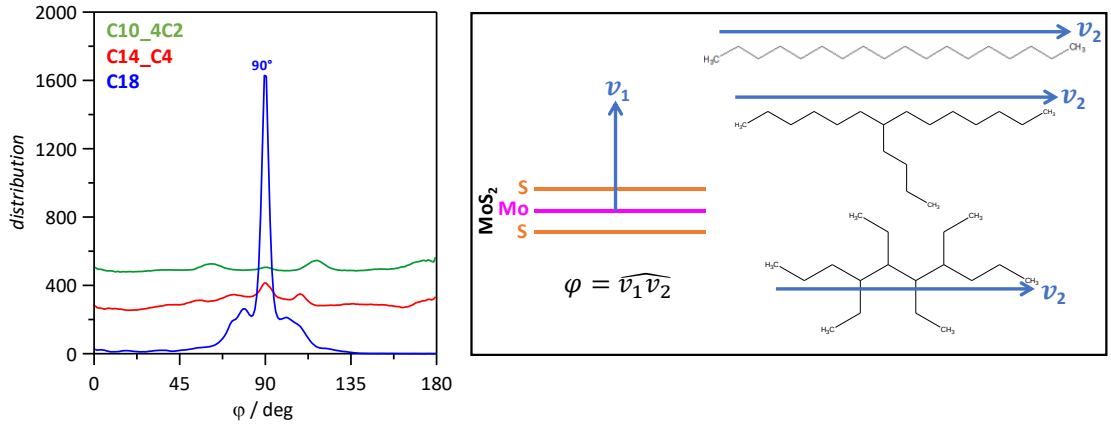

Figure 9

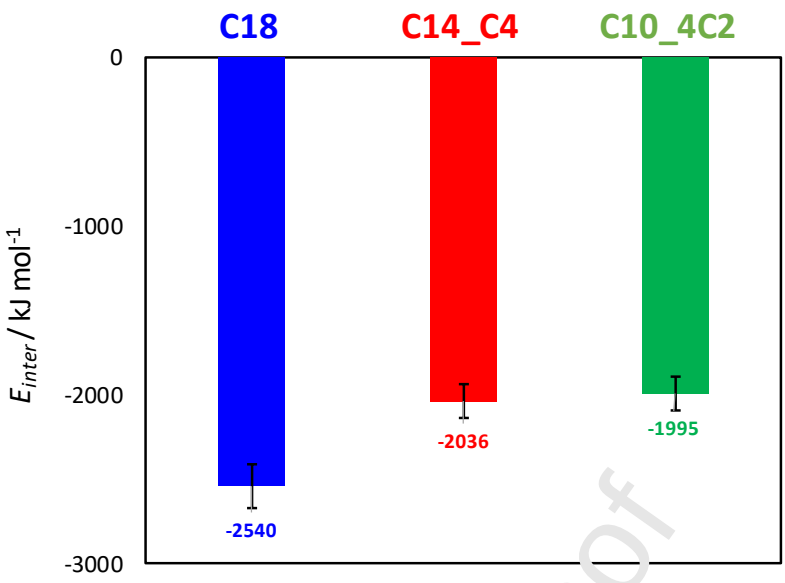

Figure 10

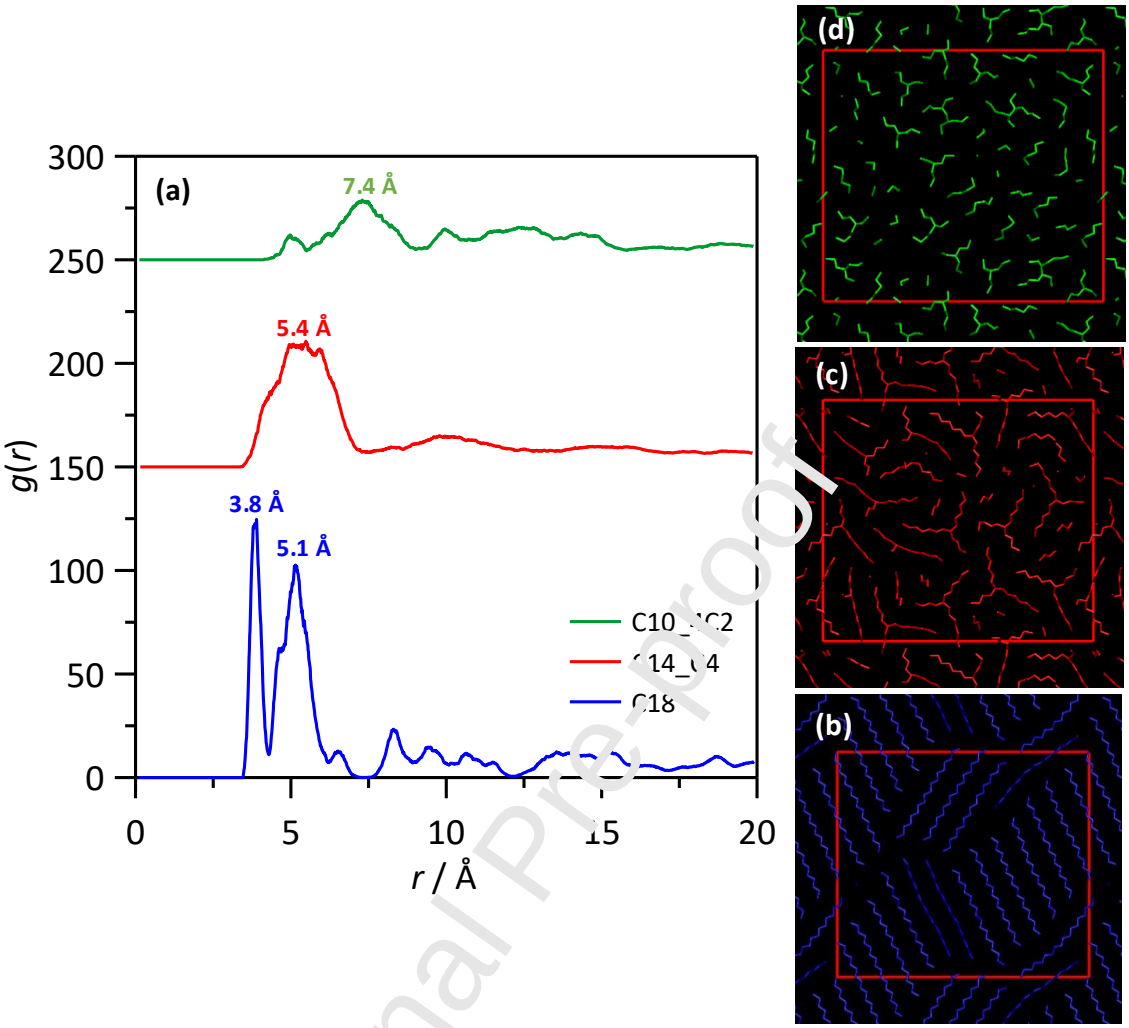

Figure 11

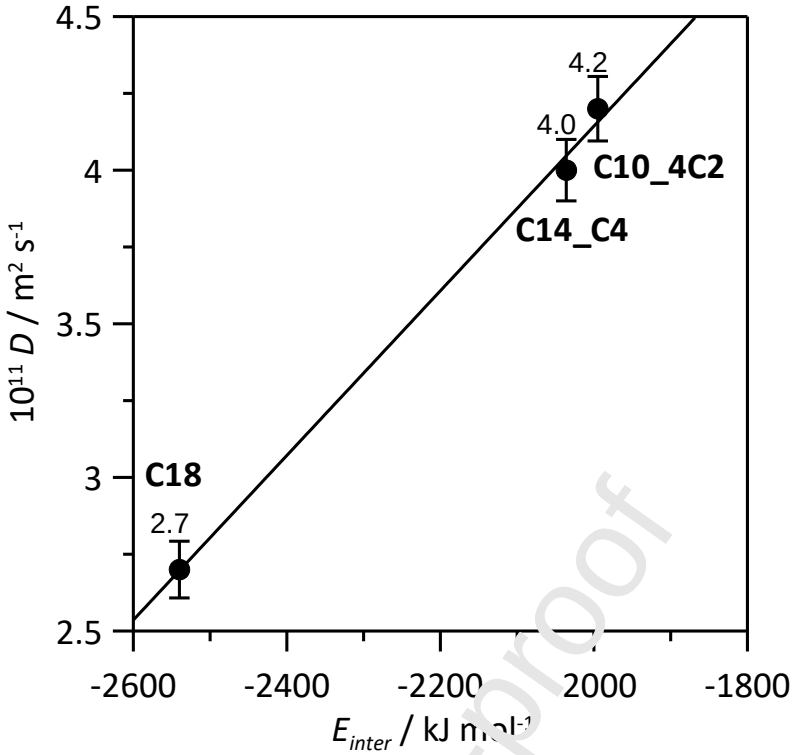

Figure 12

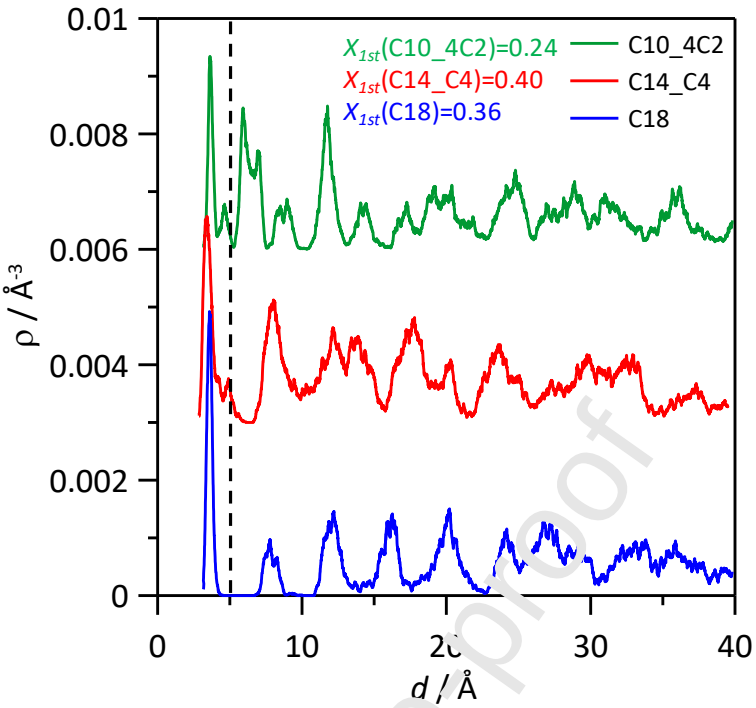

Figure 13

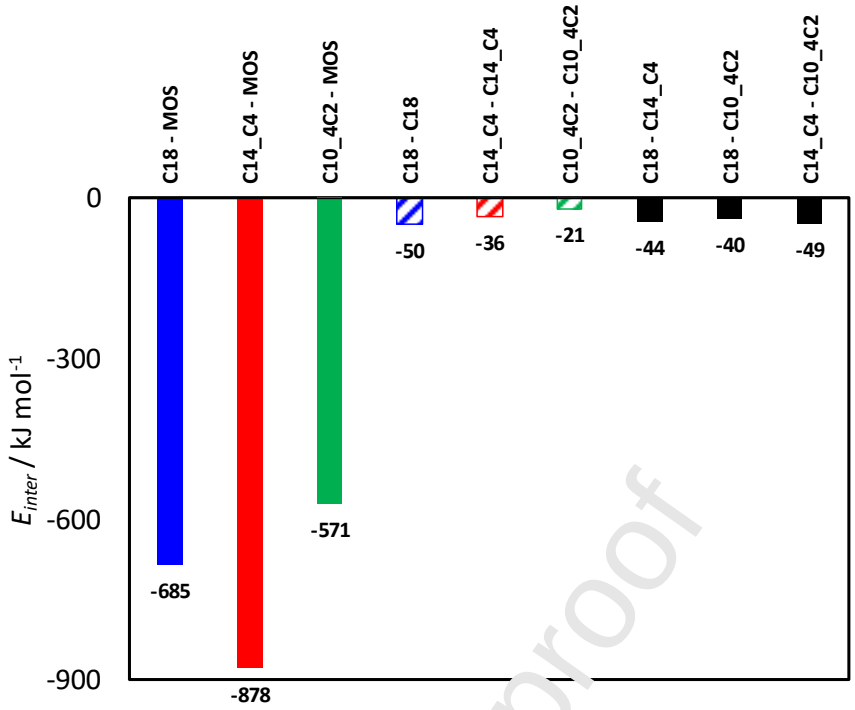

Figure 14

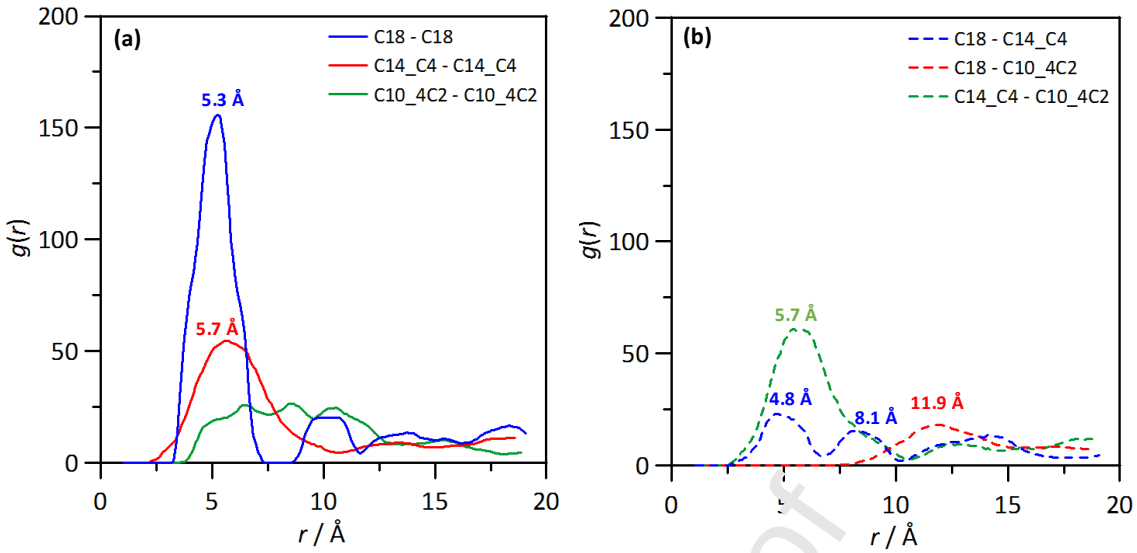

Figure 15

Highlights

- Poly-α-olefins lubricant oils
- Nanoadditives with 2D MoS_2.
- Adsorption of oils at the surface with layering and reordering.
- Cooperativity effect upon adsorption.
- Oils rearrangements in the vicinity of monolayers.

References

[1] F.A. Yunusov, A.D. Brichi, A.S. Vasilyeva, O.V. Tolochko, The influence of nano additives on tribological properties of lubricant oil. Materials Today: Proceedings (2020) DOI: j.matpr.2020.01.447

[2] A. Singh, P. Chauhan, T.G. Mamatha, A review on tribological performance of lubricants with nanoparticles additives. Materials Today Proceedings 25 (2020) 586-591.

[3] V. Srinivas, R.N. Thakur, A.K. Jain, Antiwear, antifriction, and extreme pressure properties of motor bike engine oil dispersed with molybdenum disulfide nanoparticles. J. Tribol. Trans. 60 (2017)12-19.

[4] S.B. Mousavi, S.Z. Heris, M.G. Hosseini, Experimental investigation of MoS_2/diesel oil nanofluid thermophysical and rheological properties. Int. Commun. Heat Mass. 108 (2019) 104298.

[5] M. R. Yi, C. H. Zhang, The synthesis of MoS_2 particles with different morphologies for tribological applications. Tribol. Int. 116 (2017) 285–294.

[6] M.J.G. Guimarey, A.M. Abdelkader, M.J.P. Comuñas, C. Álvarez-Lorenzo, B. Thomas, J. Fernández, M. Hadfield, Comparison between thermophysical and tribological properties of two engine lubricant additives: electrochemically exfoliated graphene and molybdenum disulfide nanoplatelets, Nanotechnology 32,(2020) 025701.

[7] G. G. Tang, J. Zhang, C. C. Liu, D. Zhang, Y. Q. Wang, H. Tang, C. Li, Synthesis and tribological properties of flower-like MoS_2 microspheres. Ceram. Int. 40 (2014) 11575–11580.

[8] S. V. Prabhakar, C. Byon, C. V. Reddy, B. Venkatesh and J. Shim, Synthesis and structural characterization of MoS2 nanospheres and nanosheets using solvothermal method, J. Mater. Sci., 2015, 50, 5024–5038.

[9] J. Guo, R.Peng, h. Du, Y. Shen, Y. Li, J. Li, G. Dong, The application of Nano-mos_2 quantum dots as liquid lubricant additive for tribological behavior improvement. Nanomaterials 10 (2020) 200.

[10] S. Xiong, D. Liang, B. Zhang, H. Wu, X. Mao, Tribological behavior of mineral and synthetic ester base oil containing MoS_2 nanoparticles. J. Disper. Sci. Technol. (2019) DOI: 10.1080/01932691.2019.1700132

[11] N. Rajendhran, S. Palanisamy, P. Periyasamy, R. Venkatachalam, enhancing of the tribological characteristics of the lubricant oils using Ni-Promoted MoS_2 nanosheets as nano-additives. Tribol. Int. 118 (2018) 314–328.

[12] Y. Xu, Y. Peng, T. You, L. Yao, J. Geng, K. Dearn, X. Hu, Nano-MoS_2 and graphene additives in oil for tribological applications. in nanotechnology in oil and gas industries: principles and applications; topics in mining, metallurgy and materials engineering; Saleh T. A., Ed.; Springer, 2018; pp 151–191.

[13] K.K. Singh, R.Prabhu, S. Choudhary, C. Pramanik, N.S. John, Effect of graphene and mos_2 flakes in industrial oils to enhance lubrication. ACS Omega 4 (2019) 14569-14578.

[14] M. Yi, C. Zhang, The synthesis of two-dimensional MoS_2 nanosheets with enhanced tribological properties as oil additives. RSC Adv. 8 (2018) 9564-9573.

[15] N. Rajendhran, S. Palanisamy, P. Periyasamy, R. Venkatachalam, Enhancing of the tribological characteristics of the lubricant oils using Ni-promoted MoS_2 nanosheets as nano-additives. Tribol. Int. 118 (2018) 314-328.

[16] S.B. Mousavi, S.Z. Heris, P. Estelle, Experimental comparison between ZnO and MoS_2 nanoparticles as additives on performance of diesel oil-based nano lubricant. Scientific Reports 10 (2010) 5813.

[17] L. Maritsa, A. Bol, S. Aparicio. Quasi-Smectic liquid crystal phase of octane in contact with 2D MoS2. Appl. Surf. Sci. (2020)

[18] S.Q. Dong, P.K. Mi, S. Xu, J. Zhang, R.D. Zhao, Preparation and characterization of single-component Poly-αolefin oil base stocks. Energy Fuels 33 (2019) 9796-9804.

[19] R. Benda, A. Plomer, P. Reboul, Polyalphaolefins — base fluids for modern heavy duty diesel oils. J. Synthetic Lubrication 15 (1998) 117-132.

[20] L.I. Kioupis, E.J. Maginn, Molecular simulation of Poly-r-olefin synthetic lubricants: impact of molecular architecture on performance properties. J. Phys. Chem. B 103 (1999) 10781-10790.

[21] L. Wu, B. Song, L.M. Keer, L. Gu, Nanoplate diffusion behavior in poly-α-olefin lubricating oil. Crystals 8 (2018) 361.

[22] J.M. Soler, E. Artacho, J.D. Gale, A. García, J. Junquera, P. Ordejón, D. Sánchez-Portal, The SIESTA method for Ab Initio order- N materials simulation. J. Phys. Condens. Matter. 2002, 14, 2745–2779.

[23] J.P. Perdew, K. Burke, M. Ernzerhof, Generalized gradient approximation made simple. Phys. Rev. Lett. 1996, 77, 3865–3868.

[24] N. Troullier, J.L. Martins, Efficient pseudopotentials for plane-wave calculations. II. operators for fast iterative diagonalization. Phys. Rev. B. 1991, 43, 8861–8869.

[25] S. Grimme, Semiempirical GGA-type density functional constructed with a long-range dispersion correction. J. Comput. Chem. 2006, 27, 1787–1799.

[26] H.J. Monkhorst, J.D. Pack, Special points for brillouin-zone integrations, Phys. Rev. B 1976, 13, 5188-5192.

[27] A.P. Lyubartsev, A.M. Laaksonen, MDynaMix - a scalable portable parallel MD simulation package for arbitrary molecular mixtures. Comput. Phys. Commun. 2000, 128, 565–589.

[28] V. Sresht, A.G. Rajan, E. Bordes, M.S. Starno, A.A.H. Pádia, D. Blankschtein, Quantitative modeling of MoS_2–solvent interfaces: predicting contact angles and exfoliation performance using molecular dynamics. J. Phys. Chem. C 2017, 121, 9022-9031.

[29] S.W.I. Siu, K. Pñukackova, R.A. Böckman, Optimization of the OPLS-AA force field for long hydrocarbons. J. Chem. Theory Comput. 8 (2012) 1459-1470.

[30] J. Koca, Z. Jirouskova, R. Svobodova Varekova, J. Vanek, Electronegativity equalization method: parameterization and validation for organic molecules using the merz-kollman-singh charge distribution scheme. J. Comput. Chem. 2009, 30, 1174–1178.

[31] M. Tuckerman, B.J. Berne, Reversible multiple time scale molecular dynamics. J. Chem. Phys. 1990, 97, 1990-2001.

[32] W. Humphrey, A. Dalke, K. Schulten, VMD - visual molecular dynamics, J. Molec. Graphics 14 (1996) 33-38.
[33] M. Brehm, B. Kirchner, TRAVIS - A free Analyzer and Visualizer for Monte Carlo and Molecular Dynamics Trajectories, J. Chem. Inf. Model. 51 (2011), 2007-2023.
[34] K.]Momma, F. Izumi, VESTA 3 for three-dimensional visualization of crystal, volumetric and morphology data, J. Appl. Crystallogr. 44 (2011) 1272-1276.
[35] Y. Wang, S. Li, J. Yi, Electronic and magnetic properties of Co doped MoS_2 monolayer. Scientific Reports 6 (2016) 24153.
[36] M.R. Islam, M.M.R. Rana, A.S.M.J. Islam, Electronic and Vibrational Properties of Single Layer Transition Metal Dichalcogenides (TMDC). 2017 2nd International Conference on Electrical & Electronic Engineering (ICEEE), Rajshahi, 2017, pp. 1-5, doi: 10.1109/CEEE.2017.8412873.